

## Research Article

# Hydrogen Sulfide Attenuates Angiotensin II-Induced Cardiac Fibroblast Proliferation and Transverse Aortic Constriction-Induced Myocardial Fibrosis through Oxidative Stress Inhibition via Sirtuin 3

Lulu Liu <sup>1,2</sup>, Weiwei Gong <sup>1</sup>, Shuping Zhang <sup>1</sup>, Jieru Shen <sup>1</sup>, Yuqin Wang <sup>1</sup>, Yun Chen <sup>1</sup>, and Guoliang Meng <sup>1</sup>

<sup>1</sup>Department of Pharmacology, School of Pharmacy, Nantong University, Nantong, 226001 Jiangsu, China

<sup>2</sup>Department of Pharmacy, Affiliated Maternity & Child Health Care Hospital of Nantong University, Nantong 226001, China

Correspondence should be addressed to Guoliang Meng; [mengguoliang@ntu.edu.cn](mailto:mengguoliang@ntu.edu.cn)

Received 18 March 2021; Revised 30 May 2021; Accepted 7 August 2021; Published 24 September 2021

Academic Editor: Joanna Lecka

Copyright © 2021 Lulu Liu et al. This is an open access article distributed under the Creative Commons Attribution License, which permits unrestricted use, distribution, and reproduction in any medium, provided the original work is properly cited.

Sirtuin 3 (SIRT3) is critical in mitochondrial function and oxidative stress. Our present study investigates whether hydrogen sulfide (H<sub>2</sub>S) attenuated myocardial fibrosis and explores the possible role of SIRT3 on the protective effects. Neonatal rat cardiac fibroblasts were pretreated with NaHS followed by angiotensin II (Ang II) stimulation. SIRT3 was knocked down with siRNA technology. SIRT3 promoter activity and expression, as well as mitochondrial function, were measured. Male wild-type (WT) and SIRT3 knockout (KO) mice were intraperitoneally injected with NaHS followed by transverse aortic constriction (TAC). Myocardium sections were stained with Sirius red. Hydroxyproline content, collagen I and collagen III,  $\alpha$ -smooth muscle actin ( $\alpha$ -SMA), and dynamin-related protein 1 (DRP1) expression were measured both *in vitro* and *in vivo*. We found that NaHS enhanced SIRT3 promoter activity and increased SIRT3 mRNA expression. NaHS inhibited cell proliferation and hydroxyproline secretion, decreased collagen I, collagen III,  $\alpha$ -SMA, and DRP1 expression, alleviated oxidative stress, and improved mitochondrial respiration function and membrane potential in Ang II-stimulated cardiac fibroblasts, which were unavailable after SIRT3 was silenced. *In vivo*, NaHS reduced hydroxyproline content, ameliorated perivascular and interstitial collagen deposition, and inhibited collagen I, collagen III, and DRP1 expression in the myocardium of WT mice but not SIRT3 KO mice with TAC. Altogether, NaHS attenuated myocardial fibrosis through oxidative stress inhibition via a SIRT3-dependent manner.

## 1. Introduction

Myocardial fibrosis is a cardiac interstitial remodeling characterized by excessive cardiac fibroblast proliferation, collagen deposition, and abnormal distribution [1, 2]. It is closely related to hypertension, chronic heart failure, hypertrophic cardiomyopathy, dilated cardiomyopathy, viral myocarditis, and many other cardiovascular diseases, which is a potential risk factor of sudden cardiac death [3–7]. However, there is no ideal strategy for the treatment of myocardial fibrosis.

Hydrogen sulfide (H<sub>2</sub>S) is considered to be the third gasotransmitter after nitric oxide (NO) and carbon monoxide (CO) [8, 9]. Endogenous H<sub>2</sub>S is catalyzed by cystathionine- $\beta$ -synthase (CBS), cystathionine- $\gamma$ -lyase (CSE), 3-mercaptopyruvate sulfurtransferase (3-MST), and so on [10, 11]. The enzymes are tissue-specific distributed in different systems. CBS is a key enzyme to produce H<sub>2</sub>S in the nervous system, while CSE is mainly in the cardiovascular system [12, 13]. Previous studies verified that H<sub>2</sub>S had protective effects against atherosclerosis, myocardial hypertrophy, myocardial ischemia-reperfusion injury, endothelial

cell damage, spermatogenic failure, and testicular dysfunction [13–21]. Moreover, we also found that H<sub>2</sub>S donor GYY4137 alleviated myocardial fibrosis in spontaneously hypertensive rats [22]. However, the detailed mechanism by which H<sub>2</sub>S attenuated cardiac fibroblast proliferation *in vitro* and myocardial fibrosis *in vivo* remains unclear.

Silent information regulator 2 (SIR2), a highly conserved NAD-dependent family histone deacetylase, serves as a cell sensor for energy utilization and metabolism regulation [23, 24]. SIR2 is widely found in mammals and consists of seven members including sirtuin 1 (SIRT1) to sirtuin 7 (SIRT7). The SIR2 family plays a role in metabolism, cancer, and other physiological and pathological processes [25, 26]. Sirtuin 3 (SIRT3) is a member of histone deacetylase III to mediate redox signaling [27]. Previous research has demonstrated that H<sub>2</sub>S was capable of increasing SIRT3 to improve mitochondrial function and attenuate oxidative stress. We found that H<sub>2</sub>S improved endothelium-dependent relaxation of aortic and mesenteric arteries in paraquat-administrated wild-type (WT) mice but not SIRT3 knockout (KO) mice [18]. H<sub>2</sub>S reduced superoxide anion production in angiotensin II- (Ang II-) stimulated cardiomyocytes, but this effect is significantly weakened after SIRT3 was knocked down. H<sub>2</sub>S protected against myocardial hypertrophy in WT mice but not SIRT3 KO mice [16]. However, it is not known whether H<sub>2</sub>S protects against cardiac fibroblast proliferation and myocardial fibrosis via SIRT3 activation.

Therefore, our present study investigates whether H<sub>2</sub>S attenuated cardiac fibroblast proliferation *in vitro* and myocardial fibrosis *in vivo* and explores the possible role of SIRT3 on the protective effects.

## 2. Materials and Methods

**2.1. Cardiac Fibroblast Culture and Treatment.** After anesthesia by isoflurane, neonatal Sprague Dawley rats aged 1 to 3 days old were killed by decapitation. Then, the left ventricular myocardium was cut into small pieces followed by digestion with trypsin in a constant temperature water bath of 37°C for 5–8 minutes. After about 10 times, all supernatants except the first time were mixed. Next, Dulbecco's modified Eagle's medium (DMEM, Wisent Inc., Montreal, QC, Canada) containing 10% fetal bovine serum (FBS, Wisent Inc., Montreal, QC, Canada) was timely added to stop excessive digestion. After centrifugation, fresh DMEM containing 10% FBS was used to resuspend the cell precipitate. After differential adhesion for 4 h, the cardiomyocytes in the medium were abandoned while confluent cardiac fibroblasts adhered to the walls. Cardiac fibroblasts of the 2<sup>nd</sup> or 3<sup>rd</sup> passage were used in our further experiments. Cells were then administrated with NaHS (50 μM, Sigma-Aldrich, St. Louis, MO), a common H<sub>2</sub>S donor, for 4 h followed by Ang II (100 nM, Sigma-Aldrich, St. Louis, MO) stimulation for an additional 24 h.

**2.2. Cell Proliferation and Hydroxyproline Content Measurement.** Cell proliferation was represented as cardiac fibroblast number enhancement, which was determined by Cell Counting Kit-8 (CCK-8, Beyotime, Shanghai, China)

as the previous study [4]. The content of hydroxyproline in the cell culture medium and in the myocardium was detected according to our previous research [4, 22].

**2.3. Luciferase Reporter Assay.** Neonatal rat cardiac fibroblasts were transfected with the SIRT3 promoter luciferase fusion plasmid using the Lipofectamine 3000 reagent (Invitrogen, Carlsbad, CA, USA), and the pRL-TK reporter plasmid served as a control reporter. After changing by the fresh medium with 10% FBS 24 h later, cells were incubated with NaHS (50 μM) for 4 h and subsequently stimulated by Ang II (100 nM) for 24 h. Next, the cell lysis buffer was added to harvest the cells. The luciferase activity was detected with a dual-luciferase reporter assay system (Promega, Madison, WI, USA). Activity of the SIRT3 promoter was assessed by the relative luciferase activities compared with pRL-TK, which was normalized to control in triplicate.

**2.4. SIRT3 RNA Interference.** After starvation for 24 h, the mixture of the SIRT3 siRNA or nonspecific control siRNA (NC siRNA) and the Lipofectamine 3000 reagent was added into cardiac fibroblasts. SIRT3 siRNA (5'-CCAUCUUUGAACUAGGCUUTT-3' and 5'-AAGCCUAGUUCAAA-GAUGGTT-3') or NC siRNA with random sequences was commercially synthesized (GenePharma, Shanghai, China). The expression of SIRT3 mRNA and protein was measured by real-time PCR and western blot, respectively, to evaluate the efficiency of SIRT3 siRNA transfection after 48 h. Some other cells were stimulated with NaHS (50 μM) for 4 h followed by Ang II (100 nM) stimulation for 24 h after siRNA was transfected into the cardiac fibroblasts.

**2.5. Immunofluorescence.** After treatment, cardiac fibroblasts were fixed by polyformaldehyde for 10 min followed by incubation with phosphate-buffered solution (PBS) containing 0.3% Triton X-100 at room temperature for 20 min. The anti- $\alpha$ -smooth muscle actin ( $\alpha$ -SMA, 1:50; Bioss, Beijing, China) or anti-dynamin-related protein 1 (DRP1, 1:50; Cell Signaling Technology, Danvers, MA, USA) antibody was added into cells at 4°C overnight followed by Cy3- or Alexa Fluor 488-conjugated IgG (1:500; Beyotime, Shanghai, China) incubation at room temperature for 2 h the next day. Nuclei were stained by DAPI (4',6-diamidino-2-phenylindole) (Beyotime, Shanghai, China). Then, cardiac fibroblasts were visualized and photographed with a fluorescence microscope (Nikon, Tokyo, Japan).

**2.6. Measurement of Superoxide Formation.** After treatment as the above description, the cardiac fibroblasts were incubated with dihydroethidium (DHE, 2 μM, in the Krebs-HEPES buffer) at 37°C without light for 30 min. The level of superoxide in cells, presented as DHE fluorescence intensity, was detected with a laser confocal microscope (Leica, Wetzlar, Germany).

**2.7. Assessment of Mitochondrial Respiration Function.** The mitochondrial respiration oxygen consumption rate (OCR) was measured as the previous description by a Seahorse Extracellular Flux Analyzer (XF-96, Seahorse Bioscience,

Santa Clara, CA, USA) [16]. After being plated in XF-96-well plates, the cardiac fibroblasts were subjected to siRNA transfection and treatment as described above. Then, the medium was changed into unbuffered DMEM containing glucose (10 mM), pyruvate (10 mM), and GlutaMAX (2 mM, Invitrogen, Carlsbad, CA, USA). Basal respiration was first obtained. After ATP synthesis was inhibited by oligomycin (Oligo, 2  $\mu$ g/mL), ATP generation during respiration was measured. Then, respiratory reserve capacity and maximal respiration were detected after uncoupler carbonyl cyanide 4-(trifluoromethoxy)phenylhydrazone (FCCP, 2  $\mu$ M) was added into the cells. Finally, rotenone and antimycin A (rot & AA, 4  $\mu$ M) were applied to completely block oxygen consumption.

**2.8. Assessment of Mitochondrial Membrane Potential ( $\Delta\psi_m$ ).** After treatment, the cardiac fibroblasts were incubated in JC-1 staining solution (Beyotime, Shanghai, China) at 37°C without light for 20 min. The level of mitochondrial membrane potential ( $\Delta\psi_m$ ) was presented as the ratio of red fluorescence by aggregates of JC-1 to green fluorescence by monomers of JC-1, which were detected with a laser confocal microscope.

**2.9. Animal Treatment.** Male 8-week-old 129S1/SvImJ WT mice and SIRT3 KO mice were fed in the Experimental Animal Center of Nantong University according to the US National Institutes of Health Guidelines for Care and Use of Laboratory Animals (approval no. NTUERLAUA-20160224).

WT mice and SIRT3 KO mice were intraperitoneally administrated by NaHS (50  $\mu$ mol·kg<sup>-1</sup>·day<sup>-1</sup>) once daily, and normal saline (NS) was given as a control. After 2 weeks, mice were intraperitoneally injected with a mixture of ketamine (100 mg·kg<sup>-1</sup>) and xylazine (5 mg·kg<sup>-1</sup>) to induce anesthesia which was confirmed by loss of reflex to toe pinching. Then, thoracotomy was performed to expose the aortic arch, and transverse aortic constriction (TAC) was carried out by tying a 6-0 nylon suture ligature against a 26-gauge needle. The needle was withdrawn immediately to form an incomplete constriction. The mice with the same operating procedures without constriction served as sham controls. After surgery, all mice went on being treated by NaHS or NS for another 2 weeks [28]. During the experiments, systolic blood pressure (SBP) was monitored by a noninvasive blood pressure analysis system (Visitech Systems, Apex, NC, USA) with the tail-cuff method every week.

**2.10. Determination of H<sub>2</sub>S Concentration in the Plasma and H<sub>2</sub>S Production in the Myocardium.** The H<sub>2</sub>S level was determined using a H<sub>2</sub>S-specific microelectrode connected to a free radical analyzer (World Precision Instruments, Sarasota, FL, USA) in light of the previous description [16]. A standard curve was obtained by the current value in different concentrations (0, 0.5, 1, 2, 4, and 8  $\mu$ M) of Na<sub>2</sub>S stock solution. H<sub>2</sub>S in the myocardium was determined in tissue homogenates. The homogenates were incubated in the assay mixture (500  $\mu$ L) containing 460  $\mu$ L tissue homogenates, 20  $\mu$ L L-cysteine (10 mmol/L), and 20  $\mu$ L pyridoxal

5'-phosphate (2 mmol/L) at 37°C in tightly sealed vials for 30 min. Then, the plasma or homogenate was dropped into the reaction solution, and there was a significant change in the current value. The H<sub>2</sub>S level in the plasma or the myocardium can be calculated according to the standard curve.

**2.11. Sirius Red Staining.** After washing 3 times, myocardial paraffin sections about 5  $\mu$ m thick were stained with saturated picric acid-Sirius red without light for 30 min. Then, the nuclei were lightly stained with Mayer's hematoxylin staining solution. Finally, the collagen deposition in the myocardium was observed and photographed with a microscope. The ratio of the perivascular collagen area (PVCA) to the luminal area (LA) was calculated to assess the degree of perivascular fibrosis in the myocardium. The collagen volume fraction (CVF), as the ratio of the interstitial collagen area to the myocardial area, was statistically analyzed to evaluate the degree of interstitial fibrosis.

**2.12. Quantitative Real-Time PCR.** Expressions of mRNA were carried out by real-time PCR following the MIQE guidelines. Extracted RNA from cardiac fibroblasts or the myocardium with the TRIzol reagent (Takara, Kyoto, Japan) was subjected to reverse transcription according to the introduction of the PrimeScript™ RT Master Mix Kit (Takara, Kyoto, Japan). Amplification of cDNA was carried out three times in the PCR System (ABI 7500, ABI, Carlsbad, CA, USA) by SYBR (Takara, Kyoto, Japan) with 18S as the housekeeping gene. All sequences of the sense primers and antisense primers are listed below (Table 1).

**2.13. Western Blots.** Protein samples extracted from cardiac fibroblasts or the left ventricular myocardium were separated by 10% or 6% sodium dodecyl sulfate- (SDS-) polyacrylamide gel electrophoresis (PAGE). Then, the proteins in the gel were transferred onto membranes of polyvinylidene fluoride (PVDF) (Millipore, Billerica, MA, USA). After the membranes were blocked with 5% nonfat milk at room temperature for 2 h, the membranes with proteins were incubated overnight with an appropriate primary antibody for anti-SIRT3 (1 : 1000; Santa Cruz Biotechnology, St. Louis, MO, USA), anti- $\alpha$ -SMA, collagen I, collagen III (1 : 1000; Bioss, Beijing, China), anti-DRP1 (1 : 1000; Cell Signaling Technology, USA), anti- $\beta$ -tubulin (1 : 3000; CMCTAG, Milwaukee, WI, USA), and anti-GAPDH (1 : 7000; Sigma-Aldrich, St. Louis, MO, USA) at 4°C. Next, membranes were incubated with horseradish peroxidase- (HRP-) labeled IgG at room temperature for 2 h. Enhanced chemiluminescence (ECL, Thermo Fisher Scientific Inc., Rockford, IL, USA) was dropped to visualize the protein blots.

**2.14. Statistical Analysis.** All data are shown as mean  $\pm$  SEM and were analyzed by one-way ANOVA followed by the Bonferroni post hoc test (STATA 15.0). The values of *P* less than 0.05 were regarded as statistically significant.

### 3. Results

**3.1. NaHS Inhibits Cell Proliferation but Enhances SIRT3 Transcription in Ang II-Stimulated Cardiac Fibroblasts.** After

TABLE 1: Sequences of primers.

Gene	Sense primer	Antisense primer
Rat SIRT1	5'-CACCAGAAAGAAGTTCACCACCAGA-3'	5'-ACCATCAAGCCGCCTACTAATCTG-3'
Rat SIRT2	5'-AGGGACAAGGAGCAGGGTTC-3'	5'-GAAGAGAGACAGCGGCAGGAC-3'
Rat SIRT3	5'-GAGGTTCTTGCTGCATGTGGTTG-3'	5'-AGTTTCCCGCTGCACAAGGTC-3'
Rat SIRT4	5'-TTGTGCCAGCAAGTCTCTC-3'	5'-GTCTCTTGGAAAGGGTGATGAAGC-3'
Rat SIRT5	5'-TCCAGCGTCCACACGAAACC-3'	5'-AACACCAGCTCCTGAGATGATGAC-3'
Rat SIRT6	5'-GCTGGAGCCCAAGGAGGAATC-3'	5'-AGTAACAAAGTGAGACCACGAGAG-3'
Rat SIRT7	5'-GAGCCAACCCTCACCCACATG-3'	5'-ACGCAGGAGGTACAGACTTCAATG-3'
Rat collagen I	5'-AGGGTCATCGTGGCTTCTCT-3'	5'-CAGGCTCTTGAGGGTAGTGT-3'
Rat collagen III	5'-AGCGGAGAATACTGGGTTGA-3'	5'-GATGTAATGTTCTGGGAGGC-3'
Mouse collagen I	5'-AAGAAGACATCCCTGAAGTCA-3'	5'-TTGTGGCAGATACAGATCAAG-3'
Mouse collagen III	5'-TTGGGATGCAGCCACCTTG-3'	5'-CGCAAAGGACAGATCCTGAG-3'
18S	5'-AGTCCCTGCCCTTTGTACACA-3'	5'-CGATCCGAGGGCCTCACTA-3'

NaHS (50  $\mu$ M) administration for 4 h followed by Ang II (100 nM) stimulation for another 24 h, cell proliferation was evaluated by cell count analysis and hydroxyproline secretion. NaHS pretreatment significantly reduced cell numbers (Figure 1(a)) and reduced hydroxyproline content in the cell culture medium (Figure 1(b)) after Ang II stimulation. These data indicated that NaHS inhibited Ang II-induced cardiac fibroblast proliferation.

Next, we assessed the possible role of SIR2 family members in the attenuated effect of NaHS on cardiac fibroblast proliferation. The mRNA expressions of all seven members, SIRT1-SIRT7, were detected by real-time PCR. SIRT1 and SIRT3 were significantly decreased after Ang II stimulation, while SIRT2, SIRT4, SIRT5, SIRT6, and SIRT7 remained unchanged. Moreover, the decreased SIRT3 was corrected by NaHS preadministration for 4 h. However, there was no significant change in SIRT1 by NaHS, suggesting that SIRT1 was possibly not critical in the inhibitory effect of NaHS on Ang II-induced cardiac fibroblast proliferation. It is worth noting that there was no alteration on SIR2 mRNA of NaHS-treated cardiac fibroblasts without Ang II stimulation (Figure 1(c)). Moreover, NaHS also increased SIRT3 promoter activity in Ang II-stimulated cardiac fibroblasts (Figure 1(d)). Taken together, NaHS enhanced SIRT3 transcription in the inhibitory effect on Ang II-induced cardiac fibroblast proliferation.

**3.2. NaHS Inhibits Ang II-Stimulated Cardiac Fibroblast Proliferation via SIRT3.** However, whether enhanced SIRT3 was crucial in the above effect remained to be elucidated. In our further study, SIRT3 was knocked down in cardiac fibroblasts by RNA interference technology. After specific SIRT3 siRNA transfection, SIRT3 was significantly reduced at both levels of mRNA and protein expressions (Figures 2(a) and 2(b)).

Then, cell numbers and hydroxyproline content of cardiac fibroblasts were assessed again after SIRT3 was silenced.

Our study showed that NaHS pretreatment significantly decreased cell numbers and reduced hydroxyproline content in Ang II-stimulated cardiac fibroblasts. However, the inhibitory effect was unavailable after SIRT3 was knocked down (Figures 2(c) and 2(d)). These results suggested that NaHS inhibited Ang II-stimulated cardiac fibroblast proliferation in a SIRT3-dependent manner.

**3.3. NaHS Suppresses Collagen Expression in Ang II-Stimulated Cardiac Fibroblasts via SIRT3.** Next, the expression of collagen I and collagen III was also examined. We found that NaHS inhibited collagen I and collagen III expressions at both the mRNA and protein levels in Ang II-stimulated cardiac fibroblasts. However, the above protective effects by NaHS were absent after SIRT3 was silenced (Figure 3). It suggested that NaHS suppressed Ang II-stimulated cardiac fibroblast collagen expression in a SIRT3-dependent manner.

**3.4. NaHS Inhibits  $\alpha$ -SMA Expression in Ang II-Stimulated Cardiac Fibroblasts via SIRT3.** The expression of  $\alpha$ -SMA is commonly regarded as a robust and sensitive marker of cardiac fibroblast differentiation [4]. The present studies found that the  $\alpha$ -SMA expression was enhanced after Ang II stimulation, which was attenuated by NaHS pretreatment. However, the above inhibitory effect of NaHS on  $\alpha$ -SMA expression was obviously blunted if SIRT3 was knocked down (Figure 4(a)). It suggested that NaHS inhibited  $\alpha$ -SMA expression in Ang II-stimulated cardiac fibroblasts via SIRT3.

**3.5. NaHS Attenuates Oxidative Stress in Ang II-Stimulated Cardiac Fibroblasts via SIRT3.** Previous studies have verified that excessive oxidative stress was a critical pathophysiological mechanism in several cardiovascular diseases including myocardial remodeling, atherosclerosis, myocardial ischemia-reperfusion injury, and diabetic cardiomyopathy

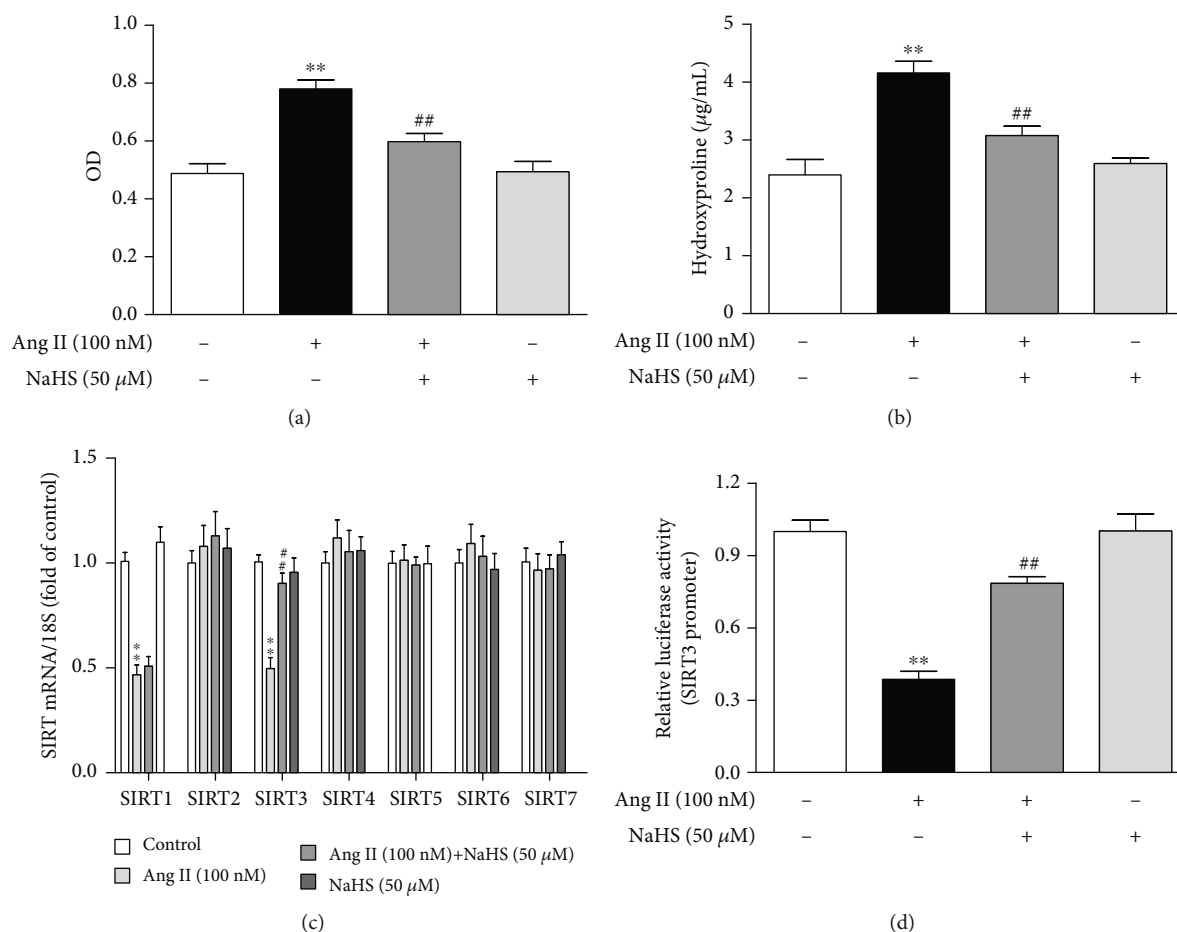


**FIGURE 1:** NaHS inhibits cell proliferation but enhances SIRT3 transcription in Ang II-stimulated cardiac fibroblasts. After pretreatment with NaHS (50  $\mu$ M) for 4 h, neonatal rat cardiac fibroblasts were stimulated by Ang II (100 nM) for 24 h. (a) The number of cardiac fibroblasts was detected with CCK-8. (b) The content of hydroxyproline in the cell culture medium was measured. (c) Expression of SIR2 family (SIRT1-7) mRNA was measured by real-time PCR. (d) After the SIRT3 promoter luciferase plasmid was transfected into cardiac fibroblasts for 24 h, cells were pretreated with NaHS (50  $\mu$ M) for 4 h followed by Ang II (100 nM) stimulation for another 24 h. Relative promoter activity of SIRT3 was detected with a dual-luciferase reporter assay system. \*\* $P < 0.01$  as compared with untreated cells; ## $P < 0.01$  as compared with Ang II alone-stimulated cells.  $n = 6$ .

[29, 30]. SIRT3, as a vital acetyl-lysine deacetylase, regulates mitochondrial function and reactive oxygen species (ROS) production [31]. Our present study found that NaHS alleviated DHE fluorescence intensity in Ang II-stimulated cardiac fibroblasts, suggesting that NaHS attenuated Ang II-stimulated ROS production. However, NaHS was no longer able to suppress DHE fluorescence intensity after SIRT3 was knocked down (Figure 4(b)). These data showed that NaHS attenuated oxidative stress in Ang II-stimulated cardiac fibroblasts via a SIRT3-dependent manner.

**3.6. NaHS Improves Mitochondrial Respiration Function and Membrane Potential in Ang II-Stimulated Cardiac Fibroblasts via SIRT3.** The above attenuated effects of NaHS on cardiac fibroblast proliferation suggested that mitochondrial function might also be improved by NaHS via SIRT3. To verify the hypothesis, the oxygen consumption rate (OCR) in Ang II-stimulated cardiac fibroblasts after NaHS administration with SIRT3 silencing was measured. Our study showed that NaHS significantly improved basal respi-

ration, ATP generation, respiratory reserve capacity, and maximal respiration in Ang II-stimulated cardiac fibroblasts, which was unavailable after SIRT3 silencing (Figures 4(c) and 4(d)). These data suggested that NaHS improved mitochondrial respiration function in Ang II-stimulated cardiac fibroblasts via SIRT3.

Next, the mitochondrial membrane potential of cardiac fibroblasts was measured by JC-1 staining. Cells with strong red fluorescence intensity indicated the normal mitochondrial membrane potential, while green fluorescence indicated a decreased one. Our results showed that NaHS increased red, but decreased green, fluorescence intensity in Ang II-stimulated cardiac fibroblasts, whereas the effect was significantly alleviated after SIRT3 was knocked down (Figure 4(e)). It suggested that NaHS improved mitochondrial membrane potential in Ang II-stimulated cardiac fibroblasts via a SIRT3-dependent manner.

**3.7. NaHS Decreases Blood Pressure but Restores  $H_2S$  Levels and SIRT3 Expression in Mice with TAC.** The above results

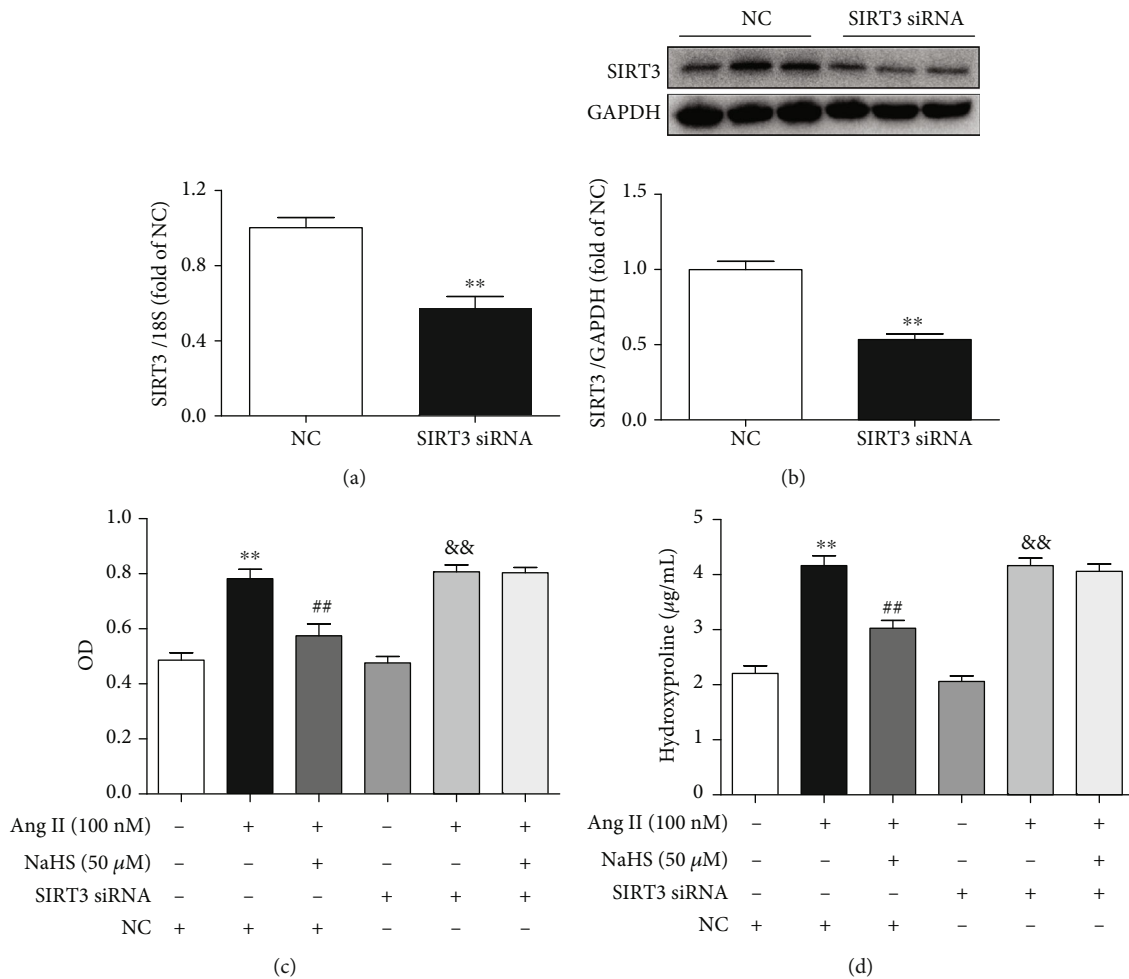


FIGURE 2: NaHS inhibits Ang II-stimulated cardiac fibroblast proliferation via SIRT3. (a, b) After SIRT3 siRNA or NC siRNA was transfected into neonatal rat myocardial fibroblasts for 48 h, expression of SIRT3 mRNA and protein was measured by real-time PCR and western blot, respectively. \*\* $P < 0.01$  as compared with cells with NC siRNA transfection.  $n = 6$ . (c) After SIRT3 siRNA or NC siRNA was transfected into cardiac fibroblasts for 24 h, the cells were pretreated with NaHS (50  $\mu$ M) for 4 h followed by Ang II (100 nM) stimulation for another 24 h. The number of cardiac fibroblasts was detected with CCK-8. (d) The content of hydroxyproline in the cell culture medium was measured. \*\* $P < 0.01$  as compared with untreated cells with NC siRNA transfection; ## $P < 0.01$  as compared with Ang II alone-stimulated cells with NC siRNA transfection; && $P < 0.01$  as compared with untreated cells with SIRT3 siRNA transfection.  $n = 6$ .

showed that NaHS inhibited Ang II-induced cardiac fibroblast proliferation in a SIRT3-dependent manner *in vitro*. Next, the role of SIRT3 in the protective effects of NaHS was investigated in mice. After TAC, SBP was significantly increased in WT and SIRT3 KO mice to the same extent in the next weeks. NaHS administration reduced SBP in both the WT and SIRT3 knockout mice (Figure 5(a)).  $H_2S$  concentration in the plasma and  $H_2S$  production in the myocardium were impaired after TAC, which was restored by the exogenous NaHS supplement in both WT mice and SIRT3 KO mice (Figures 5(b) and 5(c)). SIRT3 expression was decreased in the myocardium of WT mice after TAC, which was elevated by NaHS. And there was no SIRT3 expression in the myocardium of SIRT3 KO mice (Figure 5(d)). These data suggested that NaHS regulated blood pressure and  $H_2S$  levels regardless of the presence or absence of the SIRT3 gene.

**3.8. NaHS Ameliorates Perivascular and Interstitial Collagen Deposition in the Myocardium of WT Mice but Not SIRT3 KO Mice with TAC.** Perivascular fibrosis and interstitial fibrosis are the main manifestations of myocardial fibrosis [32]. Collagen, shown in red by Sirius red staining, was significantly suppressed by NaHS in WT mice but not SIRT3 KO mice with TAC (Figure 6(a)). Statistical analysis showed that after TAC, both the ratio of PVCA to LA and the CVF in SIRT3 KO mice were higher than that in WT mice. NaHS decreased the ratio of PVCA to LA and reduced CVF in WT mice with TAC, which was unavailable in SIRT3 KO mice (Figures 6(b) and 6(c)). It indicated that NaHS ameliorated perivascular and interstitial collagen deposition in the myocardium of WT mice but not SIRT3 KO mice with TAC.

**3.9. NaHS Reduces Collagen and  $\alpha$ -SMA Expressions in the Myocardium of WT Mice but Not SIRT3 KO Mice with**

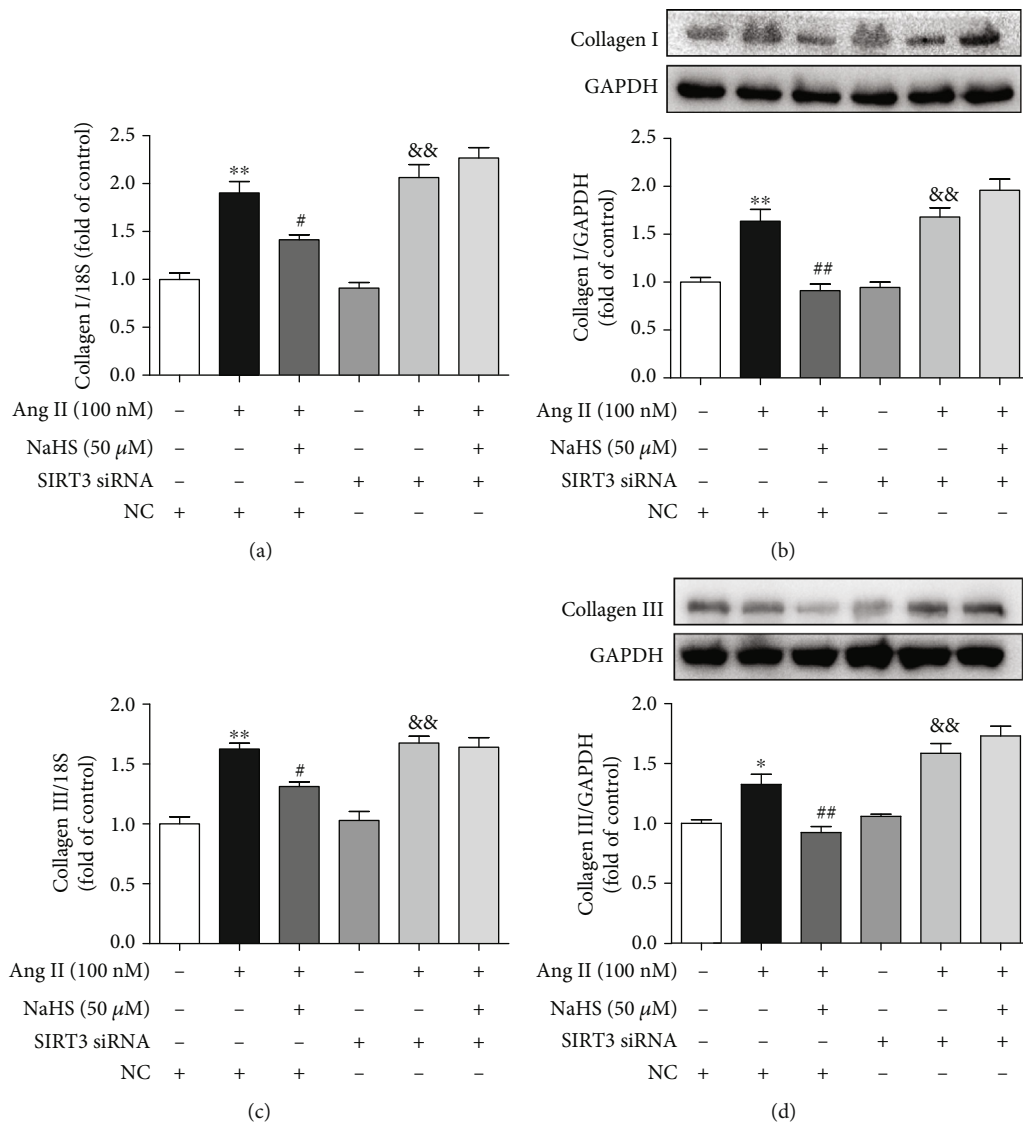
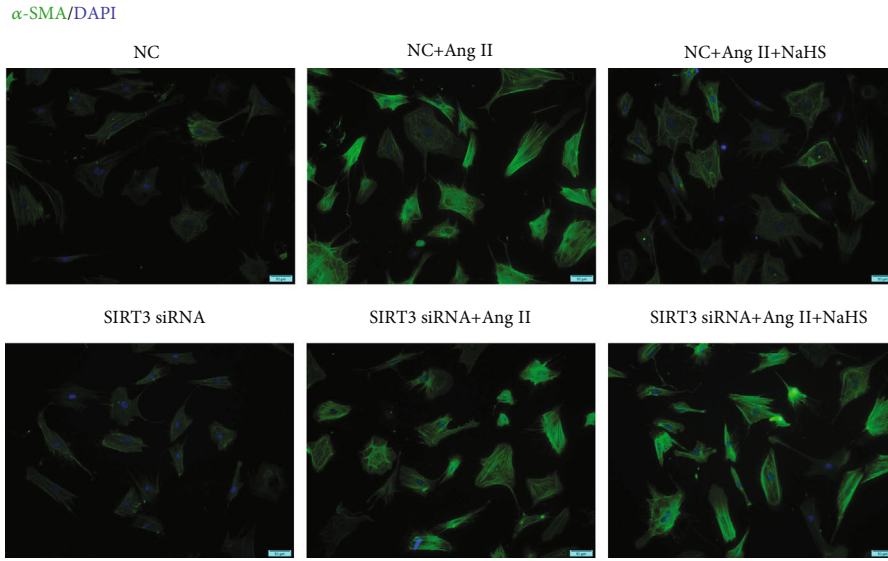


FIGURE 3: NaHS suppresses collagen expression in Ang II-stimulated cardiac fibroblasts via SIRT3. After SIRT3 siRNA or NC siRNA was transfected into neonatal rat cardiac fibroblasts for 24 h, the cells were pretreated with NaHS (50  $\mu$ M) for 4 h followed by Ang II (100 nM) stimulation for another 24 h. (a, b) Expression of collagen I mRNA and protein was measured by real-time PCR and western blot, respectively. (c, d) Expression of collagen III mRNA and protein was measured by real-time PCR and western blot, respectively. \* $P < 0.05$  and \*\* $P < 0.01$  as compared with untreated cells with NC siRNA transfection; # $P < 0.05$  and ## $P < 0.01$  as compared with Ang II alone-stimulated cells with NC siRNA transfection; && $P < 0.01$  as compared with untreated cells with SIRT3 siRNA transfection.  $n = 6$ .

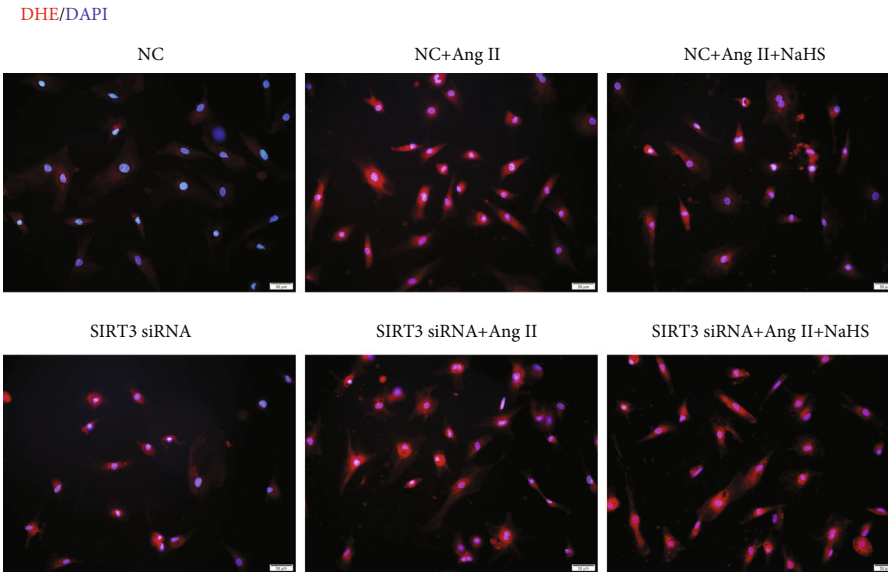
TAC. The data *in vitro* suggested that NaHS reduced collagen expression in Ang II-stimulated cardiac fibroblasts via a SIRT3-dependent manner. Next, the possible protective effect *in vivo* was further investigated. We found that after TAC, there was more hydroxyproline content and collagen expression in SIRT3 KO mice than in WT mice. NaHS reduced hydroxyproline content and collagen expression in the myocardium of WT mice with TAC. However, there was no inhibitory effect of NaHS on the above indexes in SIRT3 KO mice with TAC (Figures 7(a)–7(c)). Similarly, there was more  $\alpha$ -SMA expression in SIRT3 KO mice with TAC than in WT mice. NaHS suppressed  $\alpha$ -SMA expression in the myocardium of WT mice but not SIRT3 KO mice with TAC (Figure 7(d)). Taken together, NaHS alleviated

myocardial fibrosis in mice with TAC via a SIRT3-dependent manner.

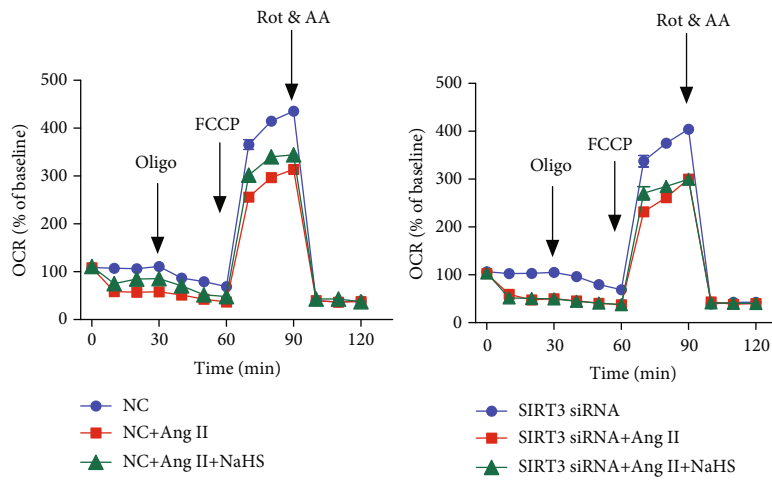
**3.10. NaHS Restores DRP1 Expression in the Cardiac Fibroblasts with Ang II Stimulation and in the Myocardium of Mice with TAC via SIRT3.** DRP1 is a protein associated with mitochondrial fission, which may induce structural damage and functional dysfunction of mitochondria [33]. Our present results showed that NaHS inhibited DRP1 expression in Ang II-stimulated cardiac fibroblasts. However, the inhibitory effect by NaHS was significantly weakened after SIRT3 was knocked down (Figures 8(a) and 8(b)). After TAC, there was more expression of DRP1 in the myocardium of SIRT3 KO mice than in WT mice. NaHS



(a)



(b)



(c)

FIGURE 4: Continued.



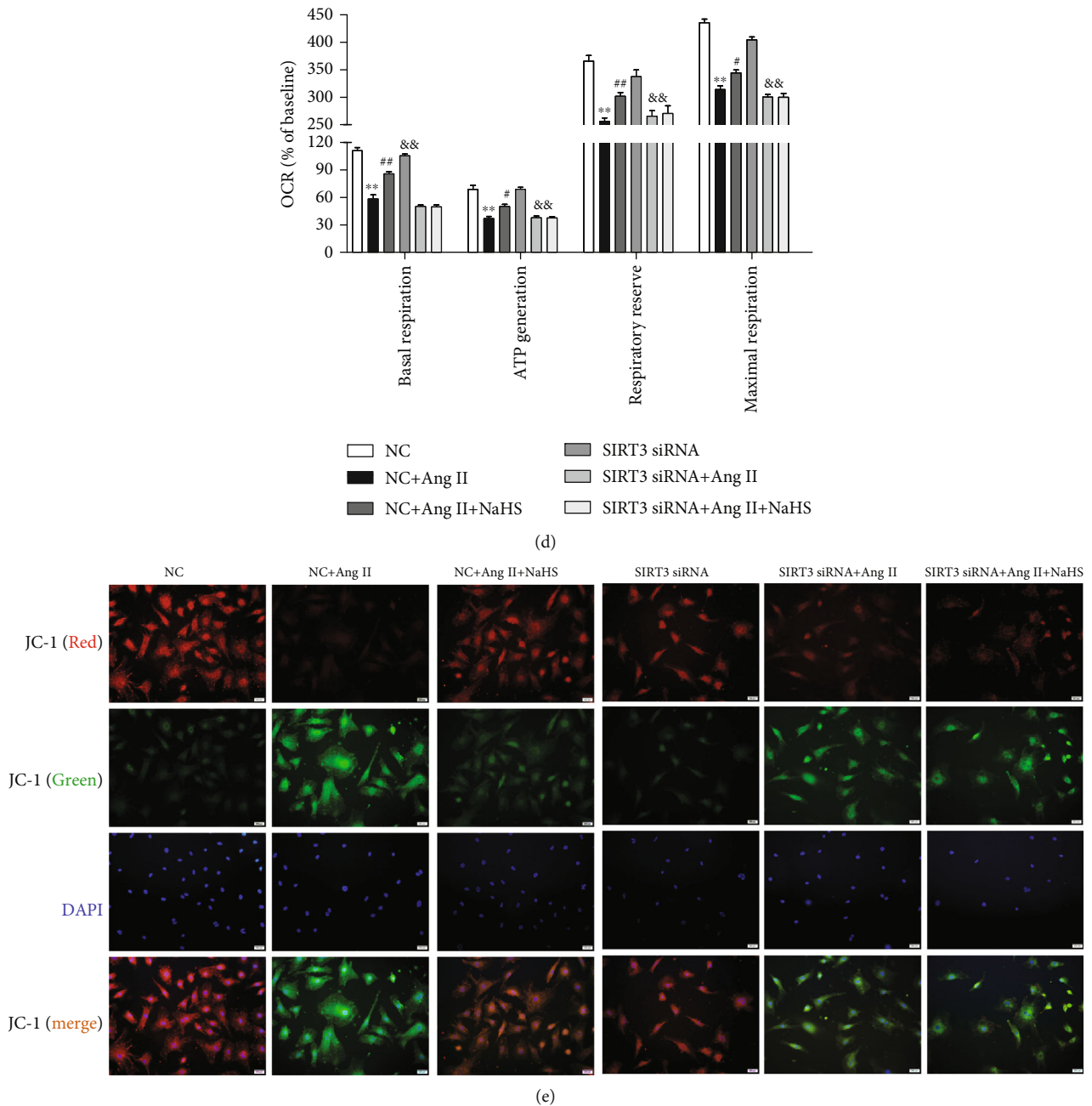


FIGURE 4: NaHS inhibits  $\alpha$ -SMA expression and oxidative stress and improves mitochondrial respiration function and membrane potential in Ang II-stimulated cardiac fibroblasts via SIRT3. After SIRT3 siRNA or NC siRNA was transfected into neonatal rat cardiac fibroblasts for 24 h, the cells were pretreated with NaHS ( $50 \mu\text{M}$ ) for 4 h followed by Ang II ( $100 \text{ nM}$ ) stimulation for another 24 h. (a) Expression of  $\alpha$ -SMA in cardiac fibroblasts was measured by immunofluorescence with Alexa Fluor 488 (green)-conjugated IgG. The nuclei were stained using DAPI (blue). Bar =  $50 \mu\text{m}$ . (b) ROS was detected with DHE staining. Bar =  $50 \mu\text{m}$ . (c) The mitochondrial respiration function of cardiac fibroblasts was measured. (d) Quantitative analysis of basal respiration, ATP generation, respiratory reserve capacity, and maximal respiratory. \*\* $P < 0.01$  as compared with untreated cells with NC siRNA transfection; # $P < 0.05$  and ## $P < 0.01$  as compared with Ang II alone-stimulated cells with NC siRNA transfection; && $P < 0.01$  as compared with untreated cells with SIRT3 siRNA transfection.  $n = 6$ . (e) Mitochondrial permeability potential was determined by JC-1 staining. Bar =  $200 \mu\text{m}$ .

suppressed DRP1 expression in the myocardium of WT mice but not SIRT3 KO mice with TAC (Figure 8(c)). All these data verified that NaHS restored DRP1 expression in the cardiac fibroblasts with Ang II stimulation and in the myocardium of mice with TAC via a SIRT3-dependent manner.

#### 4. Discussion

Myocardial fibrosis is the process of extracellular matrix remodeling to significantly increase myocardial stiffness and eventually results in heart failure and even sudden cardiac death [34]. The  $\text{H}_2\text{S}$  supplement might have protective

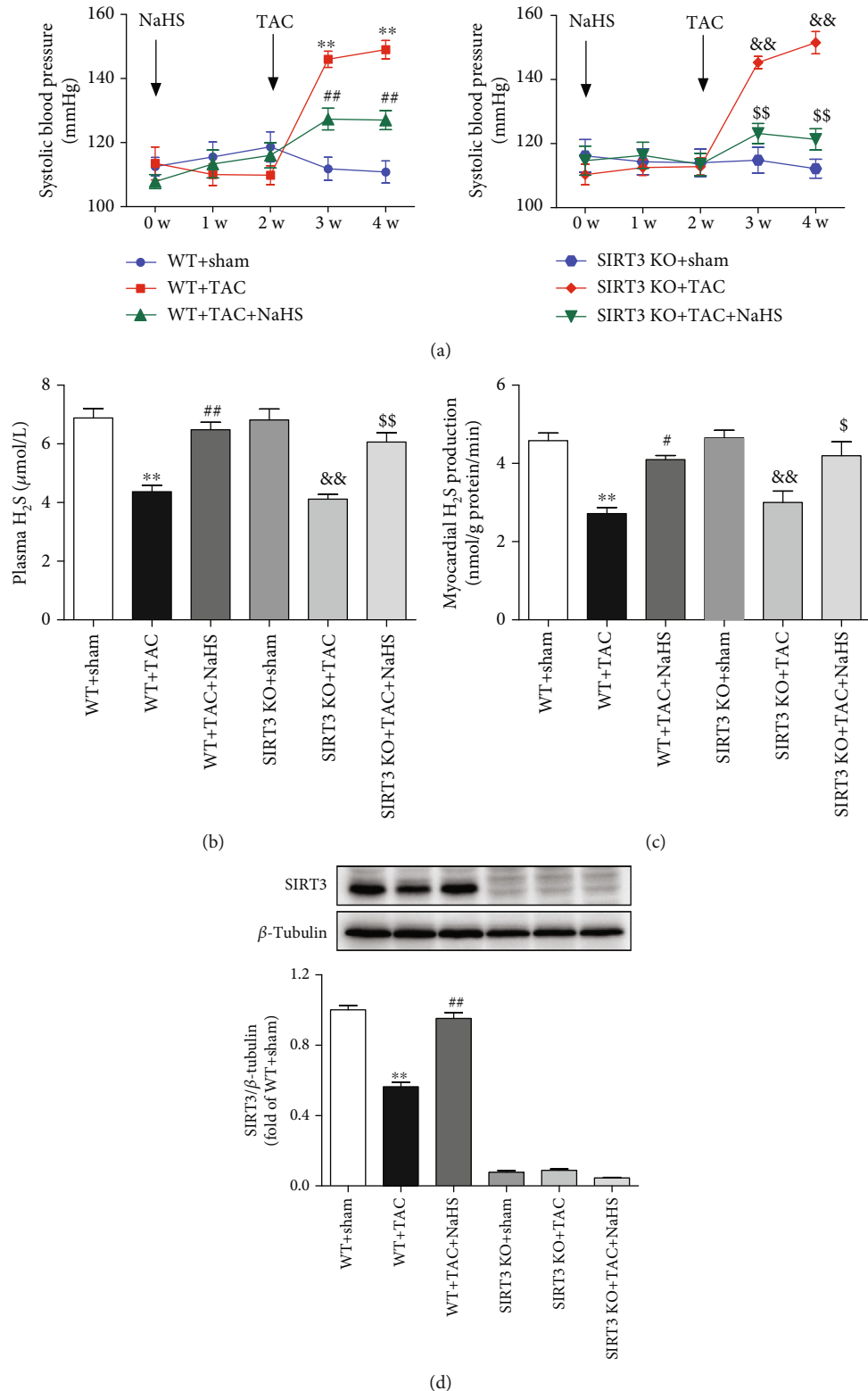


FIGURE 5: NaHS decreases blood pressure but restores H<sub>2</sub>S levels and SIRT3 expression in mice with TAC. After intraperitoneal injection by NaHS ( $50 \mu\text{mol}\cdot\text{kg}^{-1}\cdot\text{day}^{-1}$ ) or normal saline (NS) for 2 weeks, male wild-type (WT) mice and SIRT3 knockout (SIRT3 KO) mice were subjected to transverse aortic constriction (TAC) surgery. NaHS or NS was administrated for another 2 weeks. (a) The level of SBP in WT mice and SIRT3 KO mice was monitored every week after NaHS administration. (b) H<sub>2</sub>S concentration in the plasma was measured. (c) H<sub>2</sub>S production in the myocardium was detected. (d) Expression of SIRT3 protein in the myocardium was measured by western blot.  $**P < 0.01$  as compared with WT+Sham;  $*P < 0.05$  and  $##P < 0.01$  as compared with WT+TAC;  $\&\&P < 0.01$  as compared with SIRT3 KO+Sham;  $^{\$}P < 0.01$  as compared with SIRT3 KO+TAC.  $n = 6$ .

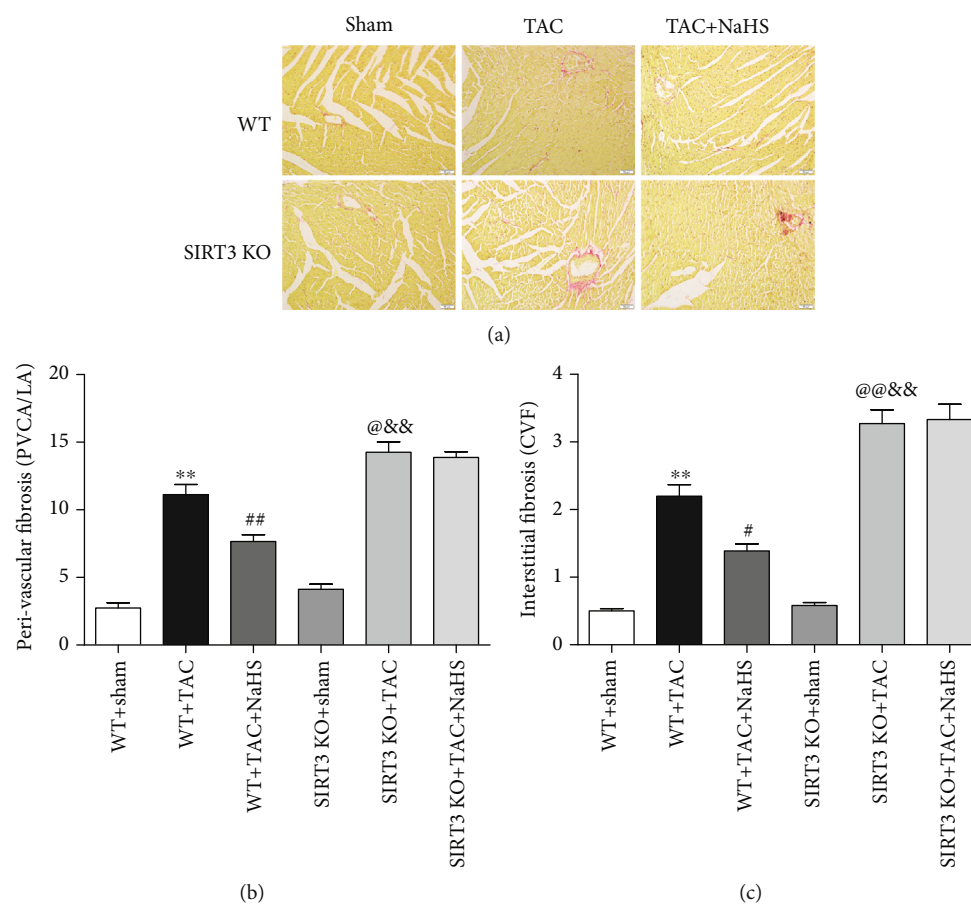


FIGURE 6: NaHS ameliorates collagen deposition in the myocardium of WT mice but not SIRT3 KO mice with TAC. After intraperitoneal injection by NaHS ( $50 \mu\text{mol}\cdot\text{kg}^{-1}\cdot\text{day}^{-1}$ ) or NS for 2 weeks, male WT mice and SIRT3 KO mice were subjected to TAC surgery. NaHS or NS was administrated for another 2 weeks. (a) Collagen deposition in the myocardium was stained with saturated picric acid-Sirius red. Bar =  $50 \mu\text{m}$ . (b) Perivascular fibrosis of the myocardium was assessed by the ratio of the perivascular collagen area (PVCA) to the luminal area (LA). (c) Interstitial fibrosis of the myocardium was assessed by the collagen volume fraction (CVF). \*\* $P < 0.01$  as compared with WT+Sham; # $P < 0.05$  or @ $P < 0.05$  and ## $P < 0.01$  or @@ $P < 0.01$  as compared with WT+TAC; && $P < 0.01$  as compared with SIRT3 KO+Sham.  $n = 6$ .

effects on myocardial ischemia-reperfusion injury, cardiac infarction, arrhythmia, cardiac hypertrophy, heart failure, and diabetic cardiomyopathy [35–37]. It is noted that  $\text{H}_2\text{S}$  suppressed cardiac fibroblast proliferation by inhibiting  $\text{K}^+$  currents or channels and blocking the transformation of atrial fibroblasts into myoblasts [38]. NaHS administration ameliorated myocardial fibrosis via inhibiting cell aging in diabetic rats [39].  $\text{H}_2\text{S}$  alleviated myocardial fibrosis and restored cardiac function in both the CSE KO and WT mice with myocardial infarction [40]. In our present experiment, we verified that NaHS inhibited cell numbers, hydroxyproline content,  $\alpha$ -SMA expression, and collagen production but enhanced SIRT3 expression in the cardiac fibroblasts and the myocardium. It suggested the inhibitory effect of  $\text{H}_2\text{S}$  on both Ang II-induced cardiac fibroblast proliferation and TAC-induced myocardial fibrosis. Moreover, NaHS equally reduced blood pressure but enhanced the  $\text{H}_2\text{S}$  level in all mice, suggesting that the failure of NaHS to inhibit myocardial fibrosis in SIRT3 KO mice is due to SIRT3 deficiency but not blood pressure.

The key role of SIRT3 in mitochondrial function has been intensively investigated. However, the possible role of SIRT3 on the protective effects of  $\text{H}_2\text{S}$  against myocardial fibrosis was unknown. Our previous research studies have shown that  $\text{H}_2\text{S}$  increased SIRT3 expression in human umbilical vein endothelial cells and cardiomyocytes [16, 18, 41]. Other groups found that  $\text{H}_2\text{S}$  improved cardiac energy substrate metabolism via SIRT3 in db/db mice [42, 43].  $\text{H}_2\text{S}$  activated SIRT3 through S-sulphydration to attenuate cisplatin-induced acute kidney injury [44].  $\text{H}_2\text{S}$  also attenuated hydrogen peroxide-induced NLR family pyrin domain-containing protein 3 (NLRP3) inflammasome activation via SIRT3 in macrophages [45]. Moreover, we verified that SIRT3 deficiency exacerbated diabetic cardiomyopathy and delayed diabetic skin wound healing [46, 47]. In our present experiment, mRNA expression of SIRT1 and SIRT3 was decreased, while other subtypes of the SIR2 family did not change significantly in cardiac fibroblasts with Ang II stimulation. Moreover, NaHS did increase SIRT3 transcription. Therefore, SIRT3 was focused on the possible pathway

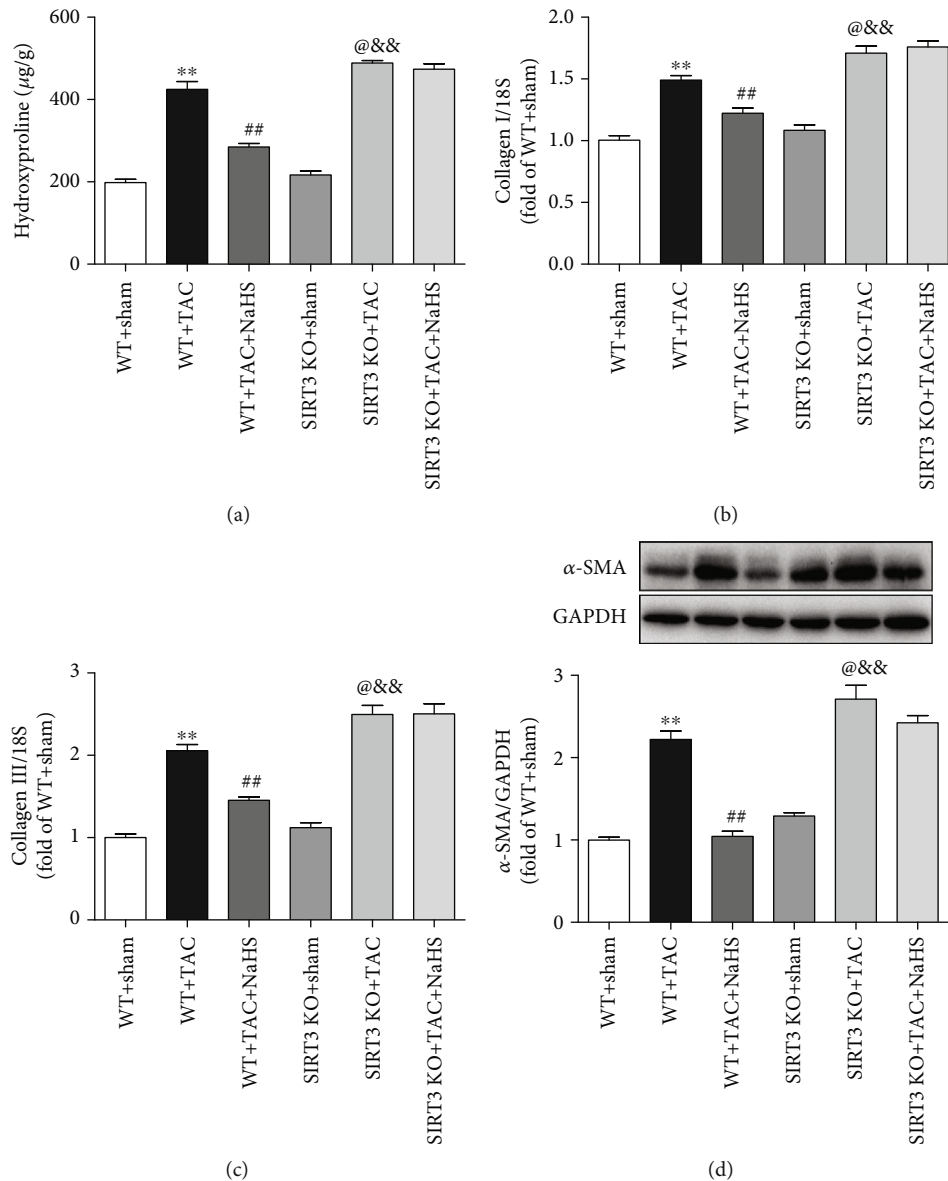
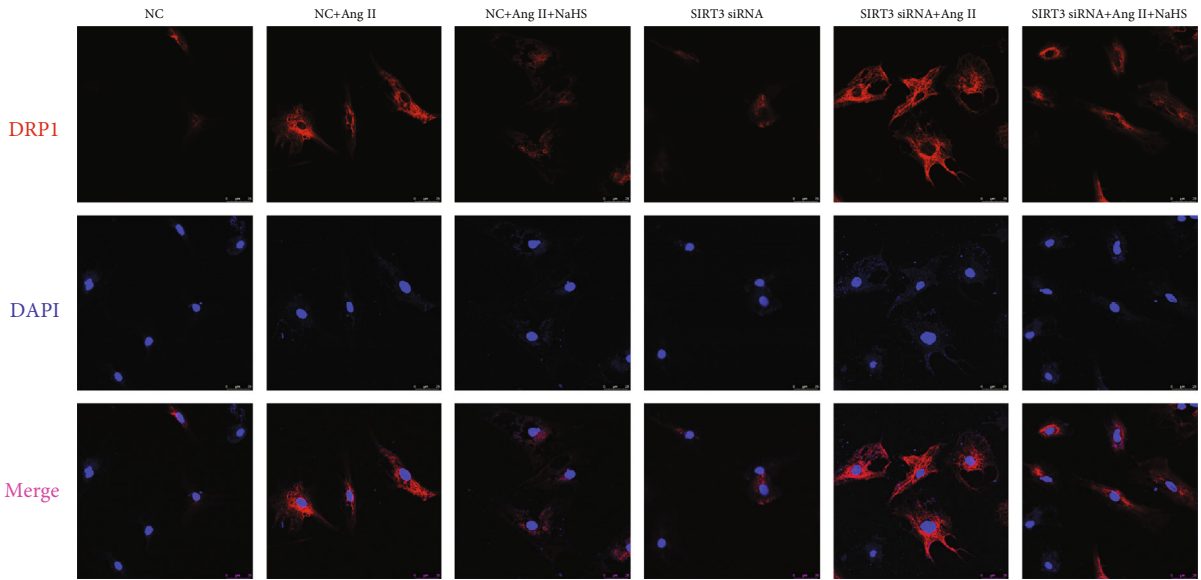


FIGURE 7: NaHS reduces collagen and  $\alpha$ -SMA expressions in the myocardium of WT mice but not SIRT3 KO mice with TAC. After intraperitoneal injection by NaHS ( $50 \mu\text{mol}\cdot\text{kg}^{-1}\cdot\text{day}^{-1}$ ) or NS for 2 weeks, male WT mice and SIRT3 KO mice were subjected to TAC surgery. NaHS or NS was administrated for another 2 weeks. (a) The content of hydroxyproline in the myocardium was measured. (b, c) Expression of collagen I and collagen III mRNA in the myocardium was measured by real-time PCR. (d) Expression of  $\alpha$ -SMA protein in the myocardium was measured by western blot. \*\* $P < 0.01$  as compared with WT+Sham; ## $P < 0.01$  or @ $P < 0.05$  as compared with WT+TAC; && $P < 0.01$  as compared with SIRT3 KO+Sham.  $n = 8$ .

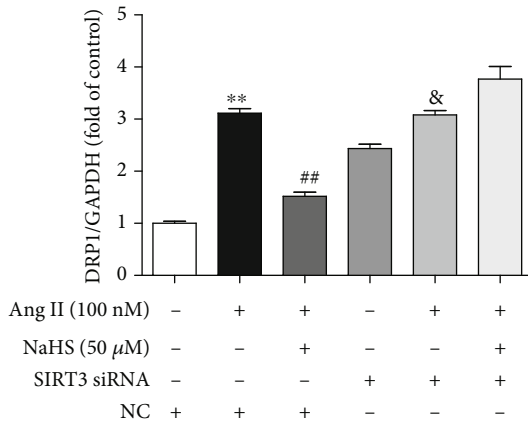
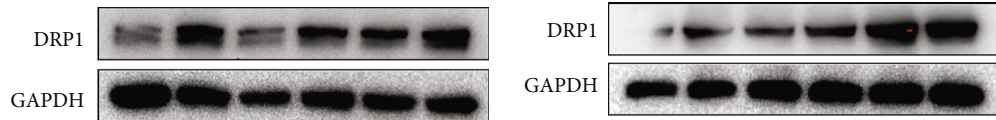
of the protective effect on myocardial fibrosis next. We found that there was more serious fibrosis in SIRT3 KO mice after TAC, suggesting the protective role of SIRT3 in TAC-induced myocardial fibrosis. Cardiac fibroblasts with SIRT3 knockdown and mice with SIRT3 deficiency further verified the protective effect on myocardial fibrosis by  $\text{H}_2\text{S}$  via a SIRT3-dependent manner. It is beneficial to clarify the mechanism of  $\text{H}_2\text{S}$  against myocardial fibrosis.

It is worth noting that the researchers know little about the detailed mechanism of how  $\text{H}_2\text{S}$  regulated SIRT3 transcription. Our previous study verified that  $\text{H}_2\text{S}$  increased activator protein 1 (AP-1) binding activity with the SIRT3

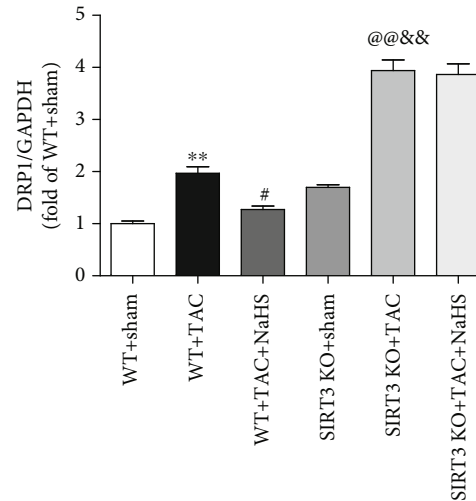
promoter to enhance SIRT3 transcription in hydrogen peroxide- ( $\text{H}_2\text{O}_2$ -) stimulated EA.hy926 endothelial cells [18]. Others demonstrated that the protective effect of  $\text{H}_2\text{S}$  in paraquat-induced liver injury was at least partly attributed to nuclear factor erythroid 2-related factor 2- (Nrf2-) dependent SIRT3 gene transcription [48].  $\text{H}_2\text{S}$  can induce S-sulfhydration on specific cysteine residues of target proteins to alter protein function and signal transduction [13]. Some studies found that  $\text{H}_2\text{S}$  S-sulfhydrated c-Jun of AP-1 to enhance the transcriptional activity on SIRT3, which contributed to decrease ROS production in  $\text{H}_2\text{O}_2$ -stimulated macrophages [45]. However, the mechanism of how  $\text{H}_2\text{S}$



(a)



(b)



(c)

**FIGURE 8: NaHS restores DRP1 expression in the cardiac fibroblasts with Ang II stimulation and in the myocardium of mice with TAC via SIRT3.** (a) After SIRT3 siRNA or NC siRNA was transfected into neonatal rat cardiac fibroblasts for 24 h, the cells were pretreated with NaHS (50 μM) for 4 h followed by Ang II (100 nM) stimulation for another 24 h. DRP1 expression in cardiac fibroblasts was detected by immunofluorescence with Cy3 (red)-conjugated IgG. The nuclei were stained using DAPI (blue). Bar = 25 μm. (b) Expression of DRP1 protein was measured by western blot. \*\**P* < 0.01 as compared with untreated cells with NC siRNA transfection; ##*P* < 0.01 as compared with Ang II alone-stimulated cells with NC siRNA transfection; &*P* < 0.05 as compared with untreated cells with SIRT3 siRNA transfection. *n* = 6. (c) After intraperitoneal injection by NaHS (50 μmol·kg<sup>-1</sup>·day<sup>-1</sup>) or NS for 2 weeks, male WT mice and SIRT3 KO mice were subjected to TAC surgery. NaHS or NS was administrated for another 2 weeks. Expression of DRP1 protein in the myocardium was measured by western blot. \*\**P* < 0.01 as compared with WT+Sham; #*P* < 0.05 or @@*P* < 0.01 as compared with WT+TAC; &&*P* < 0.01 as compared with SIRT3 KO+Sham. *n* = 6.

regulates SIRT3 transcriptional activity during myocardial fibrosis is not known at present and needs to be confirmed in further studies.

SIRT3 plays a vital role in mitochondrial biosynthesis and oxidative stress, which might be critical in the process of myocardial fibrosis [49]. Several studies also indicated

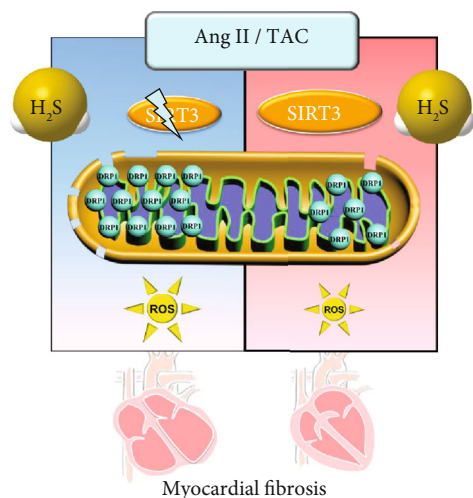


FIGURE 9: Illustration of the mechanism of protective effects on myocardial fibrosis by  $H_2S$ .  $H_2S$  enhanced SIRT3 transcription, decreased the DRP1 level, ameliorated mitochondrial membrane rupture, suppressed oxidative stress, and alleviated Ang II-induced cardiac fibroblast proliferation and TAC-induced myocardial fibrosis. However, these protective effects of  $H_2S$  were unavailable if SIRT3 was silenced in cells or deficient in mice. It suggested that  $H_2S$  attenuated myocardial fibrosis through oxidative stress inhibition via a SIRT3-dependent manner.

that  $H_2S$  was capable of attenuating oxidative stress and mitochondrial dysfunction [16, 50].  $H_2S$  inhibited oxidative stress in the myocardium of chronic heart failure [51]. Studies have shown that impaired mitochondrial permeability transition pores reduced mitochondrial membrane potential depolarization and inhibited the activation of proapoptotic proteins [52]. It has been reported that  $H_2S$  effectively improved mitochondrial membrane potential in high glucose-stimulated human umbilical vein endothelial cells [53]. This may be one of the important mechanisms for protection against mitochondrial function by  $H_2S$  [54]. We found that NaHS significantly inhibited Ang II-induced ROS production, improved mitochondrial respiration function, and restored membrane potential in a SIRT3-dependent manner. However, the detailed mechanism of the SIRT3-mediated inhibitory effect on oxidative stress by  $H_2S$  was not known well now.

Mitochondria are highly dynamic organelles undergoing cycles of fusion and fission to modulate the morphology, distribution, and function. DRP1, a key protein to regulate mitochondrial fission, is related to clearing the damaged mitochondria and maintaining the process of cellular and organ dynamics [55]. However, an excessive increase of DRP1 will break the balance between mitochondrial fusion and fission to cause mitochondrial dysfunction. Therefore, mitochondrial fission manipulated by targeting DRP1 has been an appealing therapeutic strategy for cytoprotection [56]. We found that NaHS corrected the excessive enhancement of DRP1 in both the cardiac fibroblasts with Ang II stimulation and the myocardium with TAC via a SIRT3-mediated pathway. It clarified a novel mechanism for  $H_2S$

and proposed an alternative approach for mitochondrial function protection.

In conclusion, NaHS, a  $H_2S$  donor, enhanced SIRT3 transcription and decreased the DRP1 level to possibly ameliorate mitochondrial membrane rupture, suppress oxidative stress, and alleviate Ang II-induced cardiac fibroblast proliferation and TAC-induced myocardial fibrosis. An illustration of the mechanism is outlined in Figure 9. However, these protective effects of  $H_2S$  were unavailable if SIRT3 was silenced in cells or deficient in mice. These results have shed new light on the molecular mechanism responsible for the cardioprotective effect of  $H_2S$  against myocardial fibrosis through SIRT3 activation, which might propose a novel strategy for myocardial fibrosis prevention and treatment.

## Data Availability

The data used to support the finding of this study are available from the corresponding author upon request.

## Conflicts of Interest

The authors declare that there is no conflict of interest regarding the publication of this paper.

## Authors' Contributions

Lulu Liu and Weiwei Gong contributed equally to this study.

## Acknowledgments

The work was supported by grants (81770279 and 82070280) from the National Natural Science Foundation of China, a major project of Natural Science Research in Jiangsu Higher Education Institutions (18KJA310005), the Six Talent Peaks Project in Jiangsu Province (2018-WSN-062), a Science and Technology Project of Taicang City (TC2019KJFZ02), a Science and Technology Project of Nantong City (MS22020006 and JC2019101), and a Youth Fund of Nantong Commission of Health (QA2020034).

## References

- [1] N. G. Frangogiannis, "Cardiac fibrosis: cell biological mechanisms, molecular pathways and therapeutic opportunities," *Molecular Aspects of Medicine*, vol. 65, pp. 70–99, 2019.
- [2] A. Gonzalez, E. B. Schelbert, J. Diez, and J. Butler, "Myocardial interstitial fibrosis in heart failure: biological and translational perspectives," *Journal of the American College of Cardiology*, vol. 71, no. 15, pp. 1696–1706, 2018.
- [3] P. Wang, L. Luo, Q. Shen et al., "Rosuvastatin improves myocardial hypertrophy after hemodynamic pressure overload via regulating the crosstalk of Nrf2/ARE and TGF- $\beta$ /smads pathways in rat heart," *European Journal of Pharmacology*, vol. 820, pp. 173–182, 2018.
- [4] Q. Song, L. Liu, J. Yu et al., "Dihydromyricetin attenuated Ang II induced cardiac fibroblasts proliferation related to inhibitory of oxidative stress," *European Journal of Pharmacology*, vol. 807, pp. 159–167, 2017.

- [5] F. Xu, S. Sun, X. Wang, E. Ni, L. Zhao, and W. Zhu, "GRK2 mediates arginine vasopressin-induced interleukin-6 production via nuclear Factor- $\kappa$ B signaling neonatal rat cardiac fibroblast," *Molecular Pharmacology*, vol. 92, no. 3, pp. 278–284, 2017.
- [6] M. Webber, S. P. Jackson, J. C. Moon, and G. Captur, "Myocardial fibrosis in heart failure: anti-fibrotic therapies and the role of cardiovascular magnetic resonance in drug trials," *Cardiology and Therapy*, vol. 9, no. 2, pp. 363–376, 2020.
- [7] S. Smolgovsky, U. Ibeh, T. P. Tamayo, and P. Alcaide, "Adding insult to injury - inflammation at the heart of cardiac fibrosis," *Cellular Signalling*, vol. 77, p. 109828, 2021.
- [8] Z. Li, D. J. Polhemus, and D. J. Lefer, "Evolution of hydrogen sulfide therapeutics to treat cardiovascular disease," *Circulation Research*, vol. 123, no. 5, pp. 590–600, 2018.
- [9] H. Kimura, "Signalling by hydrogen sulfide and polysulfides via protein S-sulfuration," *British Journal of Pharmacology*, vol. 177, no. 4, pp. 720–733, 2020.
- [10] X. Cao, L. Ding, Z. Z. Xie et al., "A review of hydrogen sulfide synthesis, metabolism, and measurement: is modulation of hydrogen sulfide a novel therapeutic for cancer?," *Antioxidants & Redox Signaling*, vol. 31, no. 1, pp. 1–38, 2019.
- [11] C. R. Powell, K. M. Dillon, and J. B. Matson, "A review of hydrogen sulfide (H<sub>2</sub>S) donors: chemistry and potential therapeutic applications," *Biochemical Pharmacology*, vol. 149, pp. 110–123, 2018.
- [12] G. Yang, L. Wu, B. Jiang et al., "H<sub>2</sub>S as a physiologic vasorelaxant: hypertension in mice with deletion of cystathionine gamma-lyase," *Science*, vol. 322, no. 5901, pp. 587–590, 2008.
- [13] G. Meng, S. Zhao, L. Xie, Y. Han, and Y. Ji, "Protein S-sulfhydration by hydrogen sulfide in cardiovascular system," *British Journal of Pharmacology*, vol. 175, no. 8, pp. 1146–1156, 2018.
- [14] Z. Liu, Y. Han, L. Li et al., "The hydrogen sulfide donor, GYY4137, exhibits anti-atherosclerotic activity in high fat fed apolipoprotein E(-/-) mice," *British Journal of Pharmacology*, vol. 169, no. 8, pp. 1795–1809, 2013.
- [15] L. Xie, Y. Gu, M. Wen et al., "Hydrogen sulfide induces Keap1 S-sulfhydration and suppresses diabetes-accelerated atherosclerosis via Nrf2 activation," *Diabetes*, vol. 65, no. 10, pp. 3171–3184, 2016.
- [16] G. Meng, J. Liu, S. Liu et al., "Hydrogen sulfide pretreatment improves mitochondrial function in myocardial hypertrophy via a SIRT3-dependent manner," *British Journal of Pharmacology*, vol. 175, no. 8, pp. 1126–1145, 2018.
- [17] G. Meng, Y. Xiao, Y. Ma et al., "Hydrogen sulfide regulates Krüppel-Like factor 5 transcription activity via specificity protein 1 S-sulfhydration at Cys664 to prevent myocardial hypertrophy," *Journal of the American Heart Association*, vol. 5, no. 9, 2016.
- [18] L. Xie, H. Feng, S. Li et al., "SIRT3 mediates the antioxidant effect of hydrogen sulfide in endothelial cells," *Antioxidants & Redox Signaling*, vol. 24, no. 6, pp. 329–343, 2016.
- [19] J. Wang, W. Wang, S. Li et al., "Hydrogen sulfide as a potential target in preventing spermatogenic failure and testicular dysfunction," *Antioxidants & Redox Signaling*, vol. 28, no. 16, pp. 1447–1462, 2018.
- [20] G. Meng, Y. Ma, L. Xie, A. Ferro, and Y. Ji, "Emerging role of hydrogen sulfide in hypertension and related cardiovascular diseases," *British Journal of Pharmacology*, vol. 172, no. 23, pp. 5501–5511, 2015.
- [21] Y. Qiu, Y. Wu, M. Meng et al., "GYY4137 protects against myocardial ischemia/reperfusion injury via activation of the PHLPP-1/Akt/Nrf2 signaling pathway in diabetic mice," *The Journal of Surgical Research*, vol. 225, pp. 29–39, 2018.
- [22] G. Meng, J. Zhu, Y. Xiao et al., "Hydrogen sulfide donor GYY4137 protects against myocardial fibrosis," *Oxidative Medicine and Cellular Longevity*, vol. 2015, Article ID 691070, 14 pages, 2015.
- [23] Y. Wang, J. He, M. Liao et al., "An overview of sirtuins as potential therapeutic target: structure, function and modulators," *European Journal of Medicinal Chemistry*, vol. 161, pp. 48–77, 2019.
- [24] T. Wang, Y. Wang, L. Liu et al., "Research progress on sirtuins family members and cell senescence," *European Journal of Medicinal Chemistry*, vol. 193, p. 112207, 2020.
- [25] C. K. Singh, G. Chhabra, M. A. Ndiaye, L. M. Garcia-Peterson, N. J. Mack, and N. Ahmad, "The role of sirtuins in antioxidant and redox signaling," *Antioxidants & Redox Signaling*, vol. 28, no. 8, pp. 643–661, 2018.
- [26] M. S. Elkhwanky and J. Hakkola, "Extranuclear sirtuins and metabolic stress," *Antioxidants & Redox Signaling*, vol. 28, no. 8, pp. 662–676, 2018.
- [27] W. Sun, C. Liu, Q. Chen, N. Liu, Y. Yan, and B. Liu, "SIRT3: a new regulator of cardiovascular diseases," *Oxidative Medicine and Cellular Longevity*, vol. 2018, Article ID 7293861, 11 pages, 2018.
- [28] T. Nagai, T. Anzai, H. Kaneko et al., "C-reactive protein overexpression exacerbates pressure overload-induced cardiac remodeling through enhanced inflammatory response," *Hypertension*, vol. 57, no. 2, pp. 208–215, 2011.
- [29] J. N. Peoples, A. Saraf, N. Ghazal, T. T. Pham, and J. Q. Kwong, "Mitochondrial dysfunction and oxidative stress in heart disease," *Experimental & Molecular Medicine*, vol. 51, no. 12, pp. 1–13, 2019.
- [30] Y. Zhang, P. Murugesan, K. Huang, and H. Cai, "NADPH oxidases and oxidase crosstalk in cardiovascular diseases: novel therapeutic targets," *Nature Reviews. Cardiology*, vol. 17, no. 3, pp. 170–194, 2020.
- [31] J. Zhang, H. Xiang, J. Liu, Y. Chen, R. R. He, and B. Liu, "Mitochondrial sirtuin 3: new emerging biological function and therapeutic target," *Theranostics*, vol. 10, no. 18, pp. 8315–8342, 2020.
- [32] R. B. van Heeswijk, J. A. M. Bastiaansen, J. F. Iglesias et al., "Quantification of myocardial interstitial fibrosis and extracellular volume for the detection of cardiac allograft vasculopathy," *The International Journal of Cardiovascular Imaging*, vol. 36, no. 3, pp. 533–542, 2020.
- [33] S. T. Feng, Z. Z. Wang, Y. H. Yuan et al., "Dynamin-related protein 1: a protein critical for mitochondrial fission, mitophagy, and neuronal death in Parkinson's disease," *Pharmacological Research*, vol. 151, p. 104553, 2020.
- [34] M. Gyongyosi, J. Winkler, I. Ramos et al., "Myocardial fibrosis: biomedical research from bench to bedside," *European Journal of Heart Failure*, vol. 19, no. 2, pp. 177–191, 2017.
- [35] Y. D. Wen, H. Wang, and Y. Z. Zhu, "The drug developments of hydrogen sulfide on cardiovascular disease," *Oxidative Medicine and Cellular Longevity*, vol. 2018, Article ID 4010395, 21 pages, 2018.
- [36] B. T. Hackfort and P. K. Mishra, "Emerging role of hydrogen sulfide-microRNA crosstalk in cardiovascular diseases,"

- American Journal of Physiology. Heart and Circulatory Physiology*, vol. 310, no. 7, pp. H802–H812, 2016.
- [37] H. J. Sun, Z. Y. Wu, X. W. Nie, and J. S. Bian, “Role of endothelial dysfunction in cardiovascular diseases: the link between inflammation and hydrogen sulfide,” *Frontiers in Pharmacology*, vol. 10, 2019.
- [38] J. Sheng, W. Shim, H. Wei et al., “Hydrogen sulphide suppresses human atrial fibroblast proliferation and transformation to myofibroblasts,” *Journal of Cellular and Molecular Medicine*, vol. 17, no. 10, pp. 1345–1354, 2013.
- [39] Y. Li, M. Liu, X. Song et al., “Exogenous hydrogen sulfide ameliorates diabetic myocardial fibrosis by inhibiting cell aging through SIRT6/AMPK autophagy,” *Frontiers in Pharmacology*, vol. 11, 2020.
- [40] L. J. Ellmers, E. M. Templeton, A. P. Pilbrow et al., “Hydrogen sulfide treatment improves post-infarct remodeling and long-term cardiac function in CSE knockout and wild-type mice,” *International Journal of Molecular Sciences*, vol. 21, no. 12, p. 4284, 2020.
- [41] J. Zhang, J. Yu, Y. Chen et al., “Exogenous hydrogen sulfide supplement attenuates isoproterenol-induced myocardial hypertrophy in a sirtuin 3-dependent manner,” *Oxidative Medicine and Cellular Longevity*, vol. 2018, Article ID 9396089, 17 pages, 2018.
- [42] Y. Sun, Z. Tian, N. Liu et al., “Exogenous H<sub>2</sub>S switches cardiac energy substrate metabolism by regulating SIRT3 expression in db/db mice,” *Journal of Molecular Medicine (Berlin, Germany)*, vol. 96, no. 3–4, pp. 281–299, 2018.
- [43] Y. Sun, Z. Teng, X. Sun et al., “Exogenous H<sub>2</sub>S reduces the acetylation levels of mitochondrial respiratory enzymes via regulating the NAD<sup>+</sup>-SIRT3 pathway in cardiac tissues of db/db mice,” *American Journal of Physiology. Endocrinology and Metabolism*, vol. 317, no. 2, pp. E284–E297, 2019.
- [44] Y. Yuan, L. Zhu, L. Li et al., “S-sulfhydration of SIRT3 by hydrogen sulfide attenuates mitochondrial dysfunction in cisplatin-induced acute kidney injury,” *Antioxidants & Redox Signaling*, vol. 31, no. 17, pp. 1302–1319, 2019.
- [45] Z. Lin, N. Altaf, C. Li et al., “Hydrogen sulfide attenuates oxidative stress-induced NLRP3 inflammasome activation via S-sulfhydrating c-Jun at Cys269 in macrophages,” *Biochimica et Biophysica Acta (BBA) - Molecular Basis of Disease*, vol. 1864, no. 9, pp. 2890–2900, 2018.
- [46] S. Song, Y. Ding, G. L. Dai et al., “Sirtuin 3 deficiency exacerbates diabetic cardiomyopathy via necroptosis enhancement and NLRP3 activation,” *Acta Pharmacologica Sinica*, vol. 42, no. 2, pp. 230–241, 2021.
- [47] S. Yang, M. Xu, G. Meng, and Y. Lu, “SIRT3 deficiency delays diabetic skin wound healing via oxidative stress and necroptosis enhancement,” *Journal of Cellular and Molecular Medicine*, vol. 24, no. 8, pp. 4415–4427, 2020.
- [48] Z. Liu, X. Wang, L. Li, G. Wei, and M. Zhao, “Hydrogen sulfide protects against paraquat-induced acute liver injury in rats by regulating oxidative stress, mitochondrial function, and inflammation,” *Oxidative Medicine and Cellular Longevity*, vol. 2020, Article ID 6325378, 16 pages, 2020.
- [49] A. M. Rababa'h, A. N. Guillory, R. Mustafa, and T. Hijjawi, “Oxidative stress and cardiac remodeling: an updated edge,” *Current Cardiology Reviews*, vol. 14, no. 1, pp. 53–59, 2018.
- [50] I. Andreadou, R. Schulz, A. Papapetropoulos et al., “The role of mitochondrial reactive oxygen species, NO and H<sub>2</sub>S in ischaemia/reperfusion injury and cardioprotection,” *Journal of Cellular and Molecular Medicine*, vol. 24, no. 12, pp. 6510–6522, 2020.
- [51] E. Donnarumma, S. Bhushan, J. M. Bradley et al., “Nitrite therapy ameliorates myocardial dysfunction via H<sub>2</sub>S and nuclear factor-erythroid 2-related factor 2 (Nrf2)-dependent signaling in chronic heart failure,” *Journal of the American Heart Association*, vol. 5, no. 8, 2016.
- [52] F. J. Bock and S. W. G. Tait, “Mitochondria as multifaceted regulators of cell death,” *Nature Reviews. Molecular Cell Biology*, vol. 21, no. 2, pp. 85–100, 2020.
- [53] J. Lin, X. Li, Y. Lin, Z. Huang, and W. Wu, “Exogenous sodium hydrosulfide protects against high glucose-induced injury and inflammation in human umbilical vein endothelial cells by inhibiting necroptosis via the p38 MAPK signaling pathway,” *Molecular Medicine Reports*, vol. 23, 2021.
- [54] J. Jia, Z. Wang, M. Zhang et al., “SQR mediates therapeutic effects of H<sub>2</sub>S by targeting mitochondrial electron transport to induce mitochondrial uncoupling,” *Science Advances*, vol. 6, no. 35, p. eaaz5752, 2020.
- [55] J. Y. Jin, X. X. Wei, X. L. Zhi, X. H. Wang, and D. Meng, “Drp1-dependent mitochondrial fission in cardiovascular disease,” *Acta Pharmacologica Sinica*, vol. 42, no. 5, pp. 655–664, 2021.
- [56] A. A. Rosdah, W. J. Smiles, J. S. Oakhill et al., “New perspectives on the role of Drp1 isoforms in regulating mitochondrial pathophysiology,” *Pharmacology & Therapeutics*, vol. 213, p. 107594, 2020.